within and outside tranplants. Electrode tracks were reconstructed with reference to small electrolytic lesions (Fig. 4*b*) and matched with transplantation sites made visible by pre-labelling the transplanted cells with fluorescent latex microspheres in two animals. Microscopic observation on sections stained with an antibody against glial fibrillary acidic protein (GFAP)[8], an astrocytic marker, revealed that transplanted astrocytes were localized only in the vicinity of the transplants (Fig. 4). The cells were located in a region displaying an increased immunoreactivity for GFAP (Fig. 4*b*), which reflected the reactive gliosis due to local damage by the injection. Reactive gliosis was found also in regions where non-astrocytic cells and prefrozen cells had been injected. The OD shift to the non-deprived (ipsilateral) eye was only present in the cell population situated within the transplants (Fig. 4*a*). In a second control experiment, we implanted two additional cats with cultured fibroblasts instead of astrocytes. The OD histogram from the transplanted hemispheres does not differ significantly from those obtained from the control hemispheres, which had received previously frozen cell suspension (Fig. 2).

These data show that the transplantation of astrocytes cultured from the cortices of newborn kittens is sufficient to produce OD changes induced by light deprivation in adult cats. The finding that injection of previously frozen cell suspensions and of cultured fibroblasts does not lead to OD shifts indicates that the transplantation of cells *per se*, or reactive gliosis, which is always associated with brain damage, is not sufficient to induce OD plasticity in adult cats. Reactive gliosis is mediated only to a minor extent by glial proliferation[12,13], and hence may not lead to the generation of a sufficient number of immature astrocytes. In addition, it seems unlikely that macrophages are the relevant cell type in the transplanted cultured cells because (1) the cells constituted only a minor fraction of the cultures (<2%), and (2) a high density of macrophages has to be expected in all transplanted regions because of their massive proliferation and invasion after local cortical damage[14].

How do astrocytes support visual cortical plasticity, specifically axonal sprouting and synapse elimination? Several neurotrophic factors, such as nerve growth factor, basic fibroblast growth factor and the S-100 protein, are known to be synthesized and released by astrocytes[15,16]. The ability to release trophic factors is developmentally regulated[15]. It is conceivable that such factors are released by immature astrocytes, and are selectively taken up by active terminals to support axonal sprouting or neurite extension. Furthermore, synapse elimination could be mediated by active separation of synapses by glial processes, and subsequent phagocytosis of the terminals. Such a mechanism has been observed in the normal development of the spinal chord[17–19]. A similar involvement of astrocytic processes in the regulation of synapses is found in the hypothalamo-neurohypophyseal system[20–23]. Recently it was shown that the increase of synapse density which occurs in glia-free cerebellar cultures is only reversed when astrocytes are transplanted to the cultures[24]. The temporal limitation of synapse elimination to periods when immature astrocytes are present could be due to the loss of the astrocytes' ability during maturation to undergo morphological changes and to perform phagocytosis[25,26].

The data presented here further support the hypothesis that immature glial cells are causally involved in visual cortical plasticity. The mechanisms underlying the experience-dependent change of cortical connectivity discussed above could also explain the beneficial effect of transplanted astrocytes on behavioural recovery after cortical damage[27]. It remains to be shown, however, whether astrocytes actively participate in the plastic changes proper. □

Received 20 July; accepted 2 October 1989.

1. Singer, W. in *The Neural and Molecular Bases of Learning* (eds Changeux, J. P. & Konishi, M.) 301–336 (Wiley, Chichester, 1987).
2. Le Vay, S., Stryker, M. P. & Shatz, C. J. *J. comp. Neurol.* **179,** 223–244 (1978).
3. Swindale, N. V., Vital-Durand, F. & Blakemore, C. *Proc. R. Soc.* B**213,** 435–450 (1981).
4. Kleinschmidt, A., Bear, M. F. & Singer, W. *Science* **238,** 355–358 (1987).
5. Rauschecker, J. P. & Hahn, S. *Nature* **326,** 183–185 (1987).
6. Bear, M. F. & Singer, W. *Nature* **320,** 172–176 (1986).
7. Kasamatsu, T. & Pettigrew J. D. *Science* **194,** 206–209 (1976).
8. Müller, C. M. *J. comp. Neurol.* (manuscript submitted).
9. Müller, C. M. *Glia* (manuscript submitted).
10. Hubel, D. H. & Wiesel, T. N. *J. Neurophysiol.* **28,** 1041–1059 (1965).
11. Levitt, F. B. & van Sluyters, R. C. *Devl Brain Res.* **3,** 323–327 (1982).
12. Ferrara, N., Ousley, F. & Gospodarowicz, D. *Brain Res.* **462,** 223–232 (1988).
13. Furukawa, S., Furukawa, Y., Satoyoshi, E. & Hayashi, K. *Biochem. biophys. Res. Commun.* **136,** 57–63 (1986).
14. Miyake, T., Hattori, T., Fukuda, M. & Kitamura, T. *Brain Res.* **489,** 31–40 (1989).
15. Rudge, J. S., Manthorpe, M. & Varon, S. *Devl Brain Res.* **19,** 161–172 (1985).
16. van Eldik, L. J. & Zimmer, D. B. *Brain Res.* **436,** 367–370 (1987).
17. Ronnevi, L. O. & Conradi, S. *Brain Res.* **80,** 335–339 (1974).
18. Ronnevi, L. O. *J. Neurocytol.* **6,** 487–504 (1977).
19. Ronnevi, L. O. *Cell Tiss. Res.* **189,** 203–217 (1978).
20. Tweedle, C. D. & Hatton, G. I. *Cell Tiss. Res.* **18,** 59–72 (1977).
21. Tweedle, C. D. & Hatton, G. I. *Brain Res.* **309,** 373–376 (1984).
22. Perlmutter, L. S., Tweedle, C. D. & Hatton, G. I. *Neuroscience* **12,** 503–511 (1984).
23. Perlmutter, L. S., Tweedle, C. D. & Hatton, G. I. *Neuroscience* **13,** 769–779 (1984).
24. Meshul, C. K., Seil, F. J. & Herndon, R. M. *Brain Res.* **402,** 139–145 (1987).
25. Skaper, S. D., Facci, L., Rudge, J., Katoh-Semba, R., Manthorpe, M. & Varon, S. *Devl Brain Res.* **25,** 21–31 (1986).
26. Saad, Y. A., Al-Zuhair, A. G. H. & Dawod, B. *Glia* **1,** 211–218 (1988).
27. Kesslak, J. P., Nieto-Sampedro, M., Globus, J. & Cotman, C. W. *Expl Neurol.* **92,** 377–390 (1986).
28. McCarthy, K. D. & de Vellis, J. *J. Cell Biol.* **85,** 890–902 (1980).

ACKNOWLEDGEMENTS. We are indebted to Dr H. D. Hofmann and Susanne Wallenstein for support in establishing the tissue cultures, and to Nancy Gray for improving the language.

Target size regulates calibre and myelination of sympathetic axons

James T. Voyvodic*

Department of Anatomy and Neurobiology,
Washington University Medical School, 660 S. Euclid, St Louis,
Missouri 63110, USA

AXONS in vertebrate peripheral nerves are ensheathed by Schwann cells. For some axons, this sheath consists of a single layer of glial cell cytoplasm and plasma membranes; for other axons, Schwann cells form multilayered myelin. Whether or not a Schwann cell makes myelin is determined by a signal from the axon[1,2], but the nature of this signal is not known. Here I show that sympathetic postganglionic axons, which are normally not myelinated, become myelinated when their calibre is increased as a result of increasing the size of the peripheral target they innervate. This result implies that axon calibre, which is known to be correlated with myelination[3], is in fact the crucial determinant of whether an axon becomes myelinated. Furthermore, the finding that increasing or decreasing target size causes corresponding increases or decreases in axon size indicates that axon calibre is itself regulated by retrograde signals from peripheral target tissues.

To study the effect of peripheral target size on ganglion cell axons, the relative size of a peripheral target of the superior cervical ganglion was altered during development by changing the ratio between the amount of target tissue and the number of innervating nerve cells in the ganglion. The target tissue tested in these experiments was the rat submandibular salivary gland. To make a smaller target than normal, the submandibular duct was ligated in 4-week-old rats; this results in glands weighing approximately 20% of normal when the animals reach 30 weeks of age[4–6]. These smaller glands were innervated by a normal number of superior cervical ganglion neurons (3,800 axons on average). In a second group of rats, relative target size was increased by cutting one branch of the sympathetic nerve innervating the gland at birth. When these animals were examined at 30 weeks of age, the partially denervated glands were of normal size, but were innervated by only 5–50% the normal number of sympathetic neurons[6].

* Present address: Department of Biology (Medawar Building), University College London, London WC1E 6BT, UK.

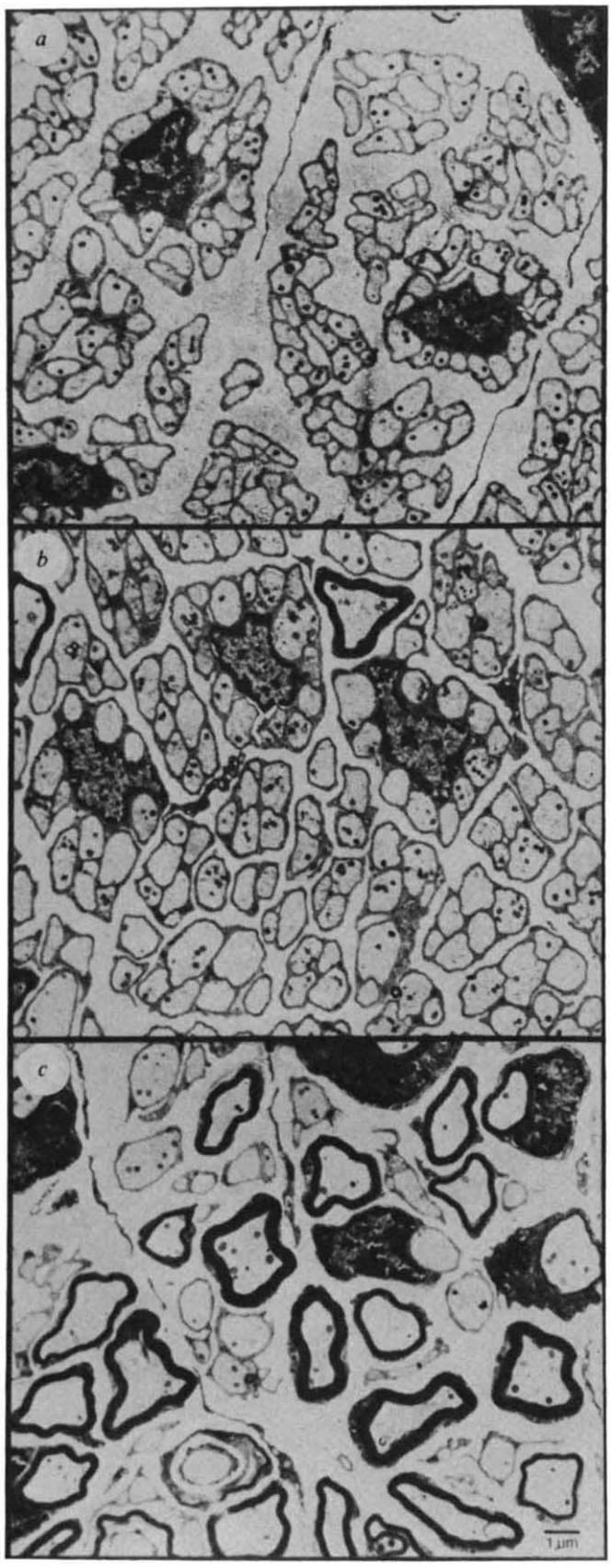

◀ FIG. 1 Effect of target size on the calibre of postganglionic sympathetic axons innervating the submandibular gland. Axons innervating: *a*, small target (submandibular duct ligated at 4 weeks of age); *b*, control target; *c*, large target (gland partially denervated at birth). All determinations were made in adult animals (30 weeks). Mean axon diameters were: *a*, 0.80 ± 0.01 μm; *b*, 1.15 ± 0.01 μm; *c*, 1.43 ± 0.02 μm. A portion of nerve midway between the gland and the external carotid nerve trunk was removed from 6-month-old animals after death; nerves were fixed by immersion and processed for electron microscopy as previously described[6]. Axon circumference was measured from electron micrographs (4,000×) using a digitizing tablet, and axon diameters were calculated as circumference/π. Scale bar is the same for all 3 panels.

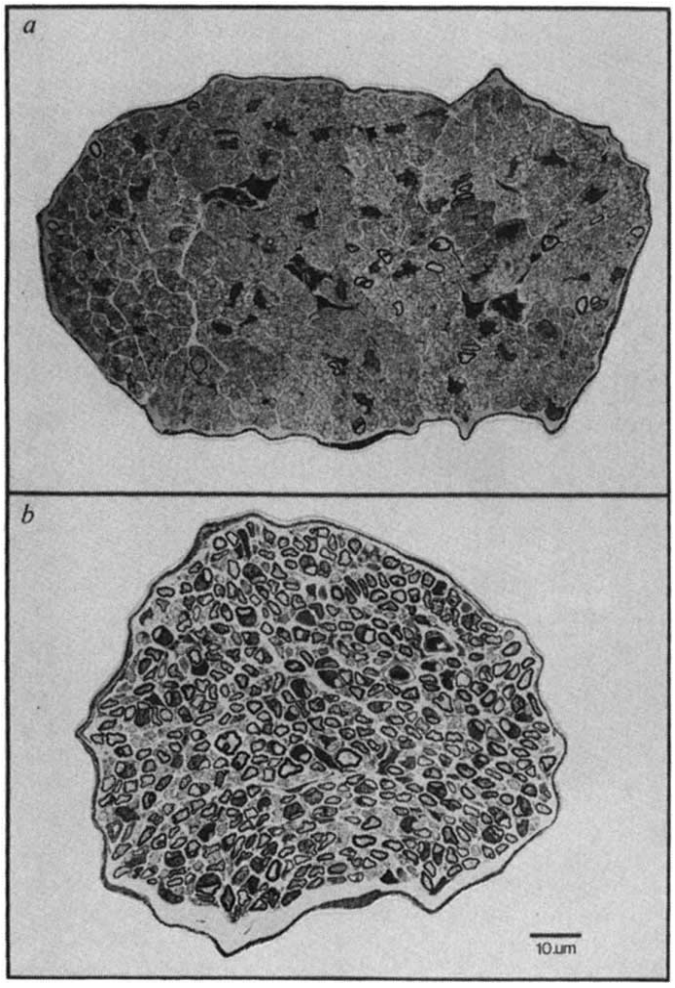

FIG. 2 Effect of increasing target size on the myelination of sympathetic axons. Electron microscope photomontages of whole postganglionic nerves innervating the submandibular gland in *a*, control (sham operated) nerve and *b*, nerve innervating relatively enlarged target (partially denervated at birth); both nerves are shown at the same magnification. In *a*, there are 3,192 unmyelinated and 25 myelinated axons; in *b*, 304 axons are unmyelinated and 386 are myelinated. Nerves were prepared for electron microscopy as described in the legend to Fig. 1. Retrograde labelling of the postganglionic nerve with horseradish peroxidase confirmed that at least 95% of the axons seen in cross-sections were axons of superior cervical ganglion neurons[6].

The postganglionic nerves carrying sympathetic axons to the submandibular gland were cut in cross-section and examined by electron microscopy (Fig. 1). Decreasing relative target size resulted in axons whose diameters were on average 31% (±0.5% s.e.m.) smaller than control axons, whereas increasing relative target size resulted in axons whose diameters were 24% (±1.7%) larger than normal. These changes in axon diameter are comparable to the magnitudes of changes previously observed in cell soma diameter and dendritic length when target size is altered under similar experimental conditions[6]. Taken together, these observations suggest that retrograde signals from the target provide a general mechanism for regulating the size of superior cervical ganglion neurons and their processes.

Target-induced changes in the size of the axon were associated with significant changes in the way in which these axons were

TABLE 1 Effect of axonal target size and preganglionic denervation on Schwann cells associated with postganglionic sympathetic axons

Experimental condition	Number of animals	Target size (μg/axon)	Total number of axons	Number of myelinated axons	Total number of Schwann cells/ cross-section
Small target	3	24 ± 4	3,596 ± 102	13 ± 1	323 ± 19
Control	4	90 ± 4	3,777 ± 90	24 ± 4	426 ± 39
Large target A	3	252 ± 56	1,620 ± 396	440 ± 189	1,111 ± 352
Large target B	2	532 ± 27	636 ± 38	291 ± 67	470 ± 75
Large target C	2	1,463 ± 155	233 ± 15	140 ± 1	233 ± 15
Preganglionic denervation					
Control target	2	73 ± 3	3,971 ± 458	19 ± 5	401 ± 22
Large target	2	954 ± 506	595 ± 292	141 ± 57	—

In the top part of the table, animals with relatively large targets were divided into 3 groups (A–C) because of the wide range of sizes produced by partial denervation (see text). Data in the lower part of the table show the effect of partial denervation of the submandibular gland for animals in which the preganglionic nerve was cut at birth[6]. The number of Schwann cells in a cross section of the nerve was estimated by dividing the total number of axons in the nerve by the number of axons per Schwann cell (calculated as described in Fig. 3.) Values are given ±s.e.m.

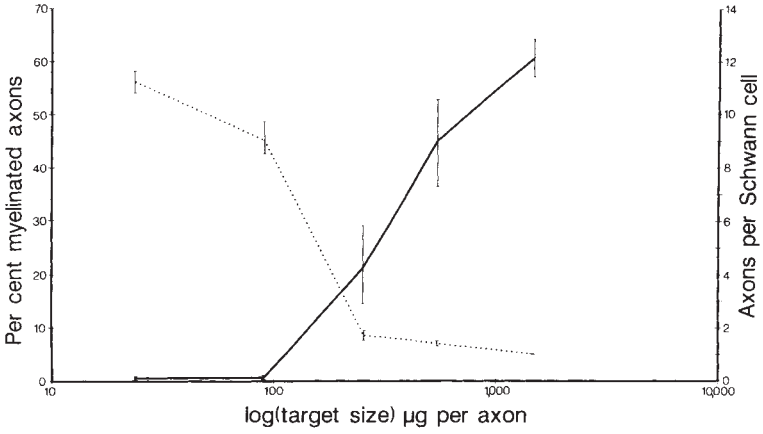

FIG. 3 Influence of target size on myelination, expressed as the percentage of axons that are myelinated (unbroken line), and on the number of axons ensheathed by each Schwann cell (dotted line). Target size is defined as the mass of the submandibular gland divided by the number of innervating sympathetic axons (counted in photomontages of whole nerves, as in Fig. 2). Each data point is the mean of values from several animals (Table 1). The number of axons ensheathed per Schwann cell was counted for each glial cell whose nucleus was visible in the plane of section; axon profiles in direct contact with the Schwann cell membrane were considered to be ensheathed by that glial cell.

ensheathed by Schwann cells. In control animals, 99.3% (±0.1% s.e.m.) of the axons in the postganglionic nerve were unmyelinated. When relative target size was increased by partial denervation, there was a dramatic increase in the number of myelinated axons in the nerve (Fig. 2). The absolute number of myelinated axons increased twelve times, on average, over the number in control nerves. Moreover, the fraction of axons that was myelinated increased progressively with increasing size of the peripheral target; for the largest targets, 60% of the axons were myelinated (Table 1; Fig. 3). When postganglionic nerves innervating experimentally enlarged targets were examined at multiple sites between the ganglion and the gland, the number of myelinated axons counted at each level was significantly above the number present in controls, indicating that these axons were myelinated along their entire length. Finally, an increase in myelination could be induced by increasing target size even if the superior cervical ganglion was denervated at birth (Table 1), suggesting that the increased myelination does not depend on electrical activity in the ganglion cells.

Two lines of evidence in this study indicate that the signal for Schwann cells to myelinate sympathetic axons is an increase in axon calibre. First, in agreement with previous reports[3,7,8], there was a clear size threshold above which axons became myelinated. Whereas 95% of unmyelinated axons were less than 1.6 μm in diameter, regardless of the experimental conditions, 90% of myelinated axons were greater than 1.6 μm in diameter. Second, even for axons below this size threshold for myelination, the number of axons ensheathed by each Schwann cell varied systematically with target size and axon calibre. Thus, when axon calibre was decreased by making a smaller target, there was no significant change in the number of myelinated axons in the postganglionic nerve, but there was a significant increase in the average number of axons ensheathed by each glial cell. On the other hand, as target size and axon calibre were increased in these experiments, the average number of axons associated with each glial cell gradually decreased (Fig. 3). This decrease was accompanied by an increase in the total number of Schwann cells present in the nerve (Table 1).

These systematic changes in the way in which Schwann cells ensheath axons of different sizes imply that Schwann cells are capable of responding to changes in axon calibre long before the axons reach the size threshold for myelination. Interestingly, the point at which Schwann cells switched from simple ensheathment to myelination was the point at which the ratio of axons to Schwann cells approached unity (Fig. 3). This relationship suggests that a Schwann cell that does not produce myelin might be triggered to begin myelination not because it detects some critical axon diameter, but rather because it reaches a point where it can no longer accommodate further axon growth by reducing the number of axons ensheathed. After Schwann cells switch to a myelinating phenotype, they once again respond to axon growth in a graded manner. In this case, however, the response is not to relinquish axons, but to add additional layers of compact myelin[7].

These results imply that there are no qualitative differences between axons that normally become myelinated and those that do not: increasing the size of a normally unmyelinated axon is sufficient to induce Schwann cells to myelinate it. These experiments also show that the calibre of peripheral axons is regulated by the size of their target. This regulation provides a mechanism by which the nervous system can continuously adjust to the growth of target tissues by modifying axonal conduction properties through retrograde signals from the target; these signals affect both axon size and myelination. □

Received 18 August; accepted 4 October 1989.

1. Weinberg, H. J. & Spencer, P. S. *Brain Res.* **133,** 363–378 (1975).
2. Aguayo, A. J. *et al J. Neurocytol.* **5,** 565–573 (1976).
3. Duncan, D. *J. comp. Neurol.* **60,** 437–472 (1934).
4. Tamarin, A. in *Secretory Mechanisms of Salivary Glands* (ed. Schneyer, L. H. & Schneyer, C. A.) 220–237 (Academic, New York, 1966).
5. Womble, M. D. & Roper, S. *J. Neurophysiol.* **58,** 276–287 (1987).

6. Voyvodic, J. T. *J. Neurosci.* **9,** 1997–2010 (1989).
7. Sanders, F. K. *Proc. R. Soc.* B**135,** 323–357 (1948).
8. Friede, R. & Samorojski, T. *J. comp. Neurol.* **130,** 223–231 (1967).

ACKNOWLEDGEMENTS. I am grateful to Dale Purves for advice and support throughout this study and to P. Newton and D. Dill for their invaluable technical assistance. I thank A. Wilson and T. Ramey for help in counting axons, and M. Raff and E. Rubin for useful comments on the manuscript. This work was supported by a NSF predoctoral fellowship and by NIH grants to D. Purves.

Membrane depolarization evokes neurotransmitter release in the absence of calcium entry

B. Hochner, H. Parnas & I. Parnas

The Otto Loewi Center, Department of Neurobiology, The Hebrew University, Jerusalem, Israel

THE discovery that Ca^{2+} is necessary for the release of neurotransmitter, the primary means by which nerve cells communicate, led to the calcium hypothesis of neutransmitter release[1–4], in which release is initiated after an action potential only by an increase in intracellular Ca^{2+} concentration near the release sites and is terminated (1–2 ms) by the rapid removal of Ca^{2+}. Since then, the calcium-voltage hypothesis has been proposed[5,6], in which the depolarization of the presynaptic terminals has two functions. First, in common with the calcium hypothesis, the Ca^{2+} conductance is increased, thereby permitting Ca^{2+} entry. Second, a conformational change is induced in a membrane molecule that renders it sensitive to Ca^{2+}, and then binding of Ca^{2+} to this active form triggers release of neurotransmitter. When the membrane is repolarized, the molecule is inactivated and release is terminated, regardless of the local Ca^{2+} concentration at that moment. This hypothesis, in contrast to the calcium hypothesis, accounts for the insensitivity of the time course of release to experimental manipulations of intracellular Ca^{2+} concentation[7–11]. Furthermore, it explains rapid termination of release after depolarization, even though Ca^{2+} concentration may still be high. Here we describe experiments that distinguish between these two hypotheses and find that our results support the calcium voltage hypothesis.

A critical test to distinguish the two hypotheses for the mechanism of neurotransmitter release separate the two effects of depolarization by raising intracellular Ca^{2+} and inducing membrane depolarization without entry of Ca^{2+}. The calcium hypothesis would then predict that the membrane depolarization would not increase release, whereas the calcium-voltage hypothesis would predict an increase in release, locked in time to the depolarizing pulse. The introduction of photosensitive Ca^{2+} chelators, the 'caged Ca^{2+}' compounds[12], makes such tests feasible. These compounds have a high affinity for Ca^{2+}, but after exposure to light, the affinity is reduced and Ca^{2+} is released. It is therefore possible to induce a phasic increase of Ca^{2+} concentration inside a presynaptic terminal without changing the membrane potential.

Zucker and Haydon[13] used a caged Ca^{2+} compound, nitr-5, to test the calcium-voltage hypothesis, and found that asynchronous transmitter release was induced by photolysis of nitr-5. In the absence of Ca^{2+} entry, as depolarization did not affect this asynchronous release, it was concluded that membrane depolarization has no direct role in the release process. The experiments underlying this conclusion, however, were made on a synapse in culture, where release is slow. It is possible that, unlike in fast synapses, a change in membrane potential does not play a part in determining the time course of release, and/or that the experimental protocol was not designed to bring out such effects (see our delay histogram, Fig. 3). We used nitr-5 to test the calcium-voltage hypothesis at a conventional fast synapse, the neuromuscular junction of the opener muscle in the first walking leg of the small crayfish *Procambarus clarkii*. It has been indicated that in this preparation membrane potential has a role in addition to the classical one of opening Ca^{2+} channels[5,14].

Figure 1 depicts the time course of the effects of pressure-injecting nitr-5 into the excitatory axon through an intracellular microelectrode placed close to the terminal[15]. Baseline responses to twin impulses (20 ms apart) recorded shortly after the intracellular penetration are shown in Fig. 1*a*. A reduction of release was apparent within three minutes after the start of injection (Fig. 1*b*). As time elapsed and more nitr-5 was injected into the axon, release was further reduced (Fig. 1*c*) until, after 18 min, it was nearly abolished (Fig. 1*d*). This reduction in release is expected because nitr-5 chelates Ca^{2+} and its K_D in darkness is close to the resting level of intracellular Ca^{2+} ($\sim 0.1\ \mu M$). These results confirm that nitr-5 is reaching the nerve terminals. At this state, the frequency of stimulation was raised to load the terminal with Ca^{2+} and to allow release to be measurable (Fig. 2*a*). A flash of light was then delivered which resulted in a transient threefold elevation of the evoked release (Fig. 2*b*). About one second after the flash, release is stabilized at a level higher than the control (compare Fig. 2*a* with Fig. 2*b*), indicating that the increase of intracellular Ca^{2+} concentration achieved by photolysis of nitr-5 is in a range that is effective for release.

Given these results, nitr-5 could be directly used to test the unique feature of the calcium-voltage hypothesis. To this end, we blocked Ca^{2+} entry using an extracellular solution essentially devoid of Ca^{2+}. Addition of EGTA damages the preparation, so we added a high concentration of Mg^{2+} (12.5 mM) both to block any possible entry of Ca^{2+} and also to substitute for Ca^{2+} in opening postsynaptic glutamate channels[16]. The effect of

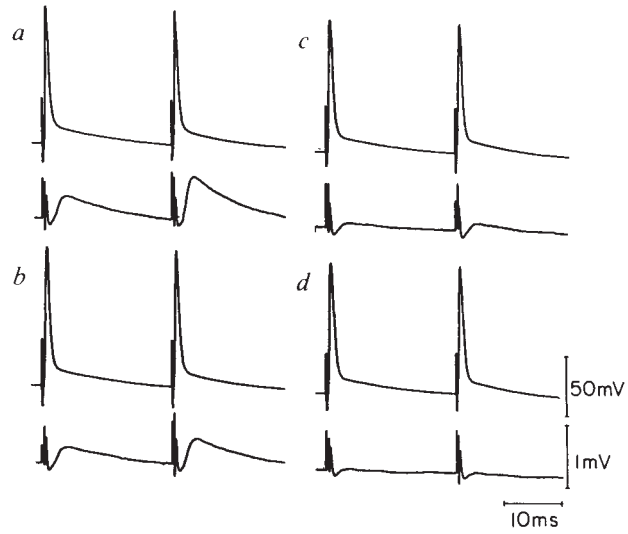

FIG. 1 *a–d*, Pressure-injection of nitr-5 reduces synaptic release. Upper traces show the axon action potential. Lower traces show the synaptic potentials. Twin impulses, 20 ms apart, were given at 3.3 Hz. Each record is an average of 50 sweeps. *a*, Control, before nitr-5 injection; and *b*, 3 min, *c*, 10 min and *d*, 18 min after beginning of injection of nitr-5. The excitatory axon was impaled distally to the main bifurcation[15] by an intracellular microelectrode, which served for recording and for pressure injection of nitr-5. The axon was stimulated by a suction electrode at its entry to the opener muscle. Another intracellular electrode recorded synaptic potentials from a muscle fibre between these two sites.

METHODS. Crayfish were supplied by Atchafalya, Louisiana. The first walking legs of small (body length 4–4.5 cm) animals were used. The bevelled microelectrode contained 50 mM nitr-5 (tetrasodium salt; Calbiochem), 35 mM $CaCl_2$, 85 mM KCl, 10 mM Tris-HCl, pH 7.4, and 0.5% fast green. For pressure injection (1 s, 10–40 psi) the Pico-Injector Model PLI-100 (Medical System) was used. Between 40–100 injection pulses were given during a period of ~30 min. E.p.s.ps were recorded with a microelectrode containing 2.5 M potassium acetate (6–10 MΩ). The preparation was perfused with a solution containing: 220 mM NaCl, 5.4 mM KCl, 12 mM $CaCl_2$, 2.5 mM $MgCl_2$, 10 mM Tris-maleate, pH 7.6, at 18–20 °C. Transilluminating light was filtered to remove wavelengths below 475 nm to avoid nitr-5 photolysis.